Technical Report

Thermal Strain Measurement Technology of Stainless Steel Exhaust System Parts

Kazunari IMAKAWA* Yoshihiro OKA
Manabu OKU

Abstract

Exhaust manifolds used as an exhaust system part of automobiles are exposed to high temperature exhaust gases discharged from engines, and are repeatedly heated and cooled along with the rotational speed of the engine. Therefore, thermal fatigue failure may occur in some cases. Currently, CAE analysis is being applied to shorten the development of exhaust manifolds and reduce costs. However, since the accuracy of the durable life prediction is not yet reliable, bench durability tests have been redone frequently. In order to improve the accuracy of the durable life prediction, it is necessary to use actual parts to accurately understand the amount of thermal strain of exhaust manifolds which occurs during the heating and cooling. Based on such a background, we performed various examinations of non-contact strain measurements under high temperatures, and developed technology to understand the thermal strain distribution on actual parts.

1. Introduction

Ferritic stainless steels are mainly used for exhaust system parts of automobiles from the viewpoint of heat and corrosion resistance. Exhaust manifolds are installed at the most upstream among the exhaust system parts and exposed to high temperature exhaust gas from the engine. They are cyclically heated and cooled as the engine speed changes. When the exhaust manifold is cyclically heated and cooled while being constrained by stays and other parts, it develops thermal strain. The accumulation of the thermal strain by this thermal cycling eventually causes the thermal fatigue failure of the exhaust manifold. We have developed steels for exhaust manifolds with thermal fatigue life improved by increasing high-temperature strength. Examples are the NSSC™ HR-1 (14Cr-1Mn-1Si-0.4Nb-0.1Cu),[1] NSSC EM-3 (18Cr-1Mn-2Mo-0.65Nb-0.2Cu),[2] NSSC EM-C (17Cr-1.4Cu-Nb-Ti),[3] and NSSC 429NF (14Cr-1.4Cu-Ti).[4]

Automobile manufacturers widely employ computer aided engineering (CAE) to reduce the lead time and cost of exhaust manifold development. They predict the thermal fatigue life of exhaust manifolds as determined by an engine bench test from the amount of thermal strain calculated by thermal stress analysis.[5] The CAE analysis can identify the fracture position from the heat strain concentration region. Because the absolute value of the thermal strain is not sufficiently accurate, the CAE analysis and engine bench testing must often be recreated. It is strongly required to improve the accuracy of the life prediction of thermal fatigue by the CAE analysis.

To improve the accuracy of the life prediction of thermal fatigue, it is necessary to accurately grasp the amount of thermal strain produced in actual exhaust manifolds during thermal cycling. High-temperature strain gauges are usually used to measure the strain of high-temperature parts. Because the high-temperature strain gauges are installed by welding, it is necessary to calibrate the amount of strain by strain relief annealing of the strain gauge welds. This necessity limits the use of high-temperature strain gauges. Also, the high-temperature strain gauges are only a few millimeters in length, are restricted as to their mounting position, and cannot measure the thermal strain in minute regions. It is thus considered difficult to measure the thermal strain in actual exhaust manifolds with high-temperature strain gauges.

Given the above situation, we started to develop the technology to accurately grasp the amount of thermal strain produced in exhaust system parts during thermal cycling by using a non-contact strain measurement unit. In this report, we describe the accuracy verification results of non-contact thermal strain measurement and the measurement results of thermal strain in actual exhaust manifolds.

* Senior Researcher, Materials Reliability Research Lab., Steel Research Laboratories, R & D Laboratories, Nippon Steel Corporation
20-1 Shintomi, Futtsu City, Chiba Pref. 293-8511

2. Experimental Methods

2.1 Thermal cycle simulator

To measure the thermal strain in the exhaust manifold, its thermal cycling must be simulated from room temperature to a high temperature close to 800°C. We conducted tests by using a thermal fatigue tester with high-frequency induction heating and a thermal cycle simulator made in-house.

Figure 1 schematically illustrates the thermal cycle simulator. Conventionally, the combustion gas from an engine or a burner was used for the thermal cycling of an exhaust manifold. With this method, it was difficult to control the air-fuel ratio and combustion temperature. Enormous cost and management effort were required to ensure safety. The thermal cycle simulator made in-house consists of a blower to draw in air and four electric heaters to heat the air. The blower was designed to control and adjust the air flow rate by arbitrarily setting the inverter frequency. To increase the contact area between the air discharged from the blower and the spiral Kanthal wires of the electric heaters, the spiral Kanthal wires were spiraled again. This made it possible to set the maximum exhaust gas temperature at 1050°C or more at the outlet of the electric heaters. In addition, temperature control could be switched between the parallel control of 2 to 4 heaters and the single control of the individual heaters. The spacing between the heaters was made changeable. The thermal cycle simulator could thus conduct thermal cycling tests on samples of various shapes from assembled exhaust manifolds to pipe dummies.

Figure 2 shows an example of mounting an exhaust manifold sample. A water-cooled flange was made so that the water flow rate could be adjusted to simulate the cooling of an engine block. The exhaust manifold sample was fastened to the water-cooled flange with an arbitrary torque. The exhaust manifold in Fig. 2 was assembled with random black and white spots applied with heat-resistant spray paints for non-contact strain measurement as described later.

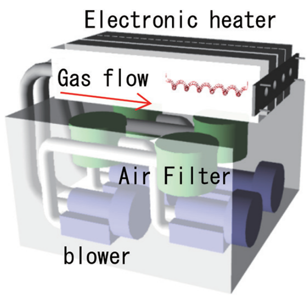

Fig. 1 Schematic diagram of thermal cycle simulator

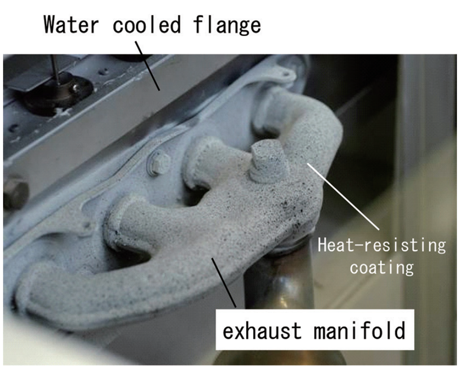

Fig. 2 Exhaust manifold mounting method

Figure 3 shows the exhaust gas temperature measured at the outlet of each heater. The heater outlet exhaust gas control conditions were a thermal cycling rate of about 2.4°C/s, an upper limit temperature of 1050°C, and a constant temperature time of 10 min. Some delay is observed in the time to reach the upper and lower constant temperatures as indicated by the arrows in Fig. 3. Thermal cycling in each heater is accurately simulated with a maximum outlet exhaust gas temperature of 1050°C.

2.2 Non-contact strain measurement method

To measure the strain distribution in the exhaust manifold, it is necessary to select a method for measuring the thermal strain in a non-contact manner and over a wide range. A measurement method suitable for strain measurement during heating was studied by using commercially available non-contact strain measurement units. A laser beam non-contact strain measurement unit shines a slit laser light beam onto the sample surface, receives the reflected laser beam with a CCD camera, and measures the shape and strain of the sample. Red hot surfaces could not be measured and it was difficult to measure the strain during heating. A measurement unit that irradiates a fringe pattern from a projector could not measure red hot surfaces either like the previous laser beam unit. It is also difficult to measure the strain during heating. A non-contact strain measurement unit that uses the digital image correlation (DIC) method captures random dots placed on the sample surface with two high-resolution digital cameras and three-dimensionally grasps the sample surface. Random dots on red hot surfaces could also be measured as far as the random dots were recognizable. The unit could also take pictures through heat-resistant glass, prevent radiant heat from the heated sample, and measure safely. **Figure 4** shows the principle of measuring the movement amount and thermal expansion amount of the sample by the DIC method. Sample surface shape data captured with the two cameras before and after heating are analyzed to calculate the movement amount and the strain amount. The sample can be simultaneously shot from multiple directions. Partially overlapping areas can be shot and the obtained analysis images can be connected. In this way, this unit can make measurements over a wide range.

According to the above study results, we selected the DIC method (hereinafter referred to as the DIC system) as our non-contact strain measurement method.

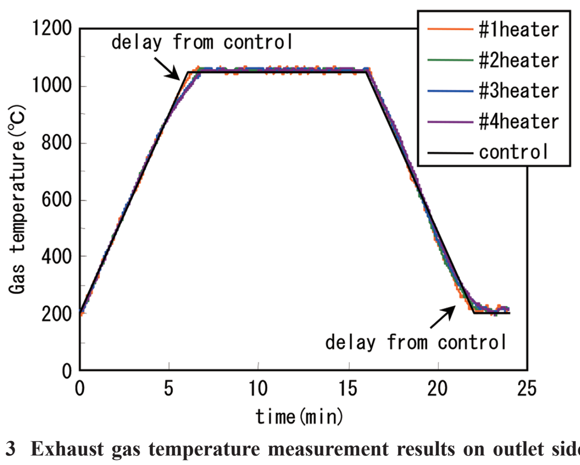

Fig. 3 Exhaust gas temperature measurement results on outlet side of each heater

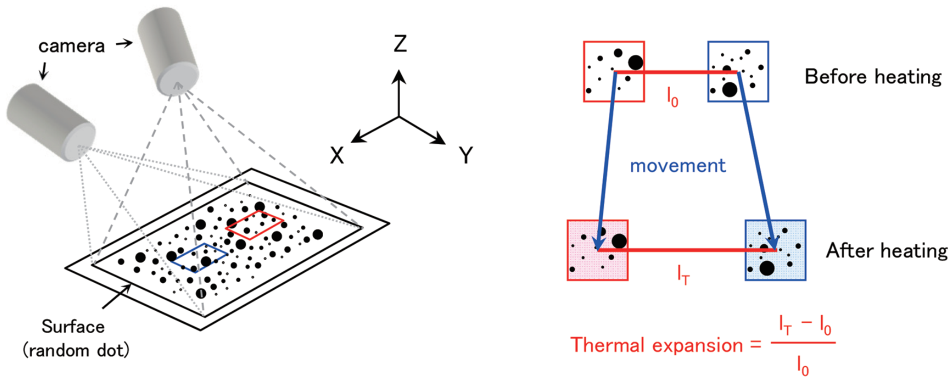

Fig. 4 Movement amount and thermal expansion amount measurement principle in DIC method

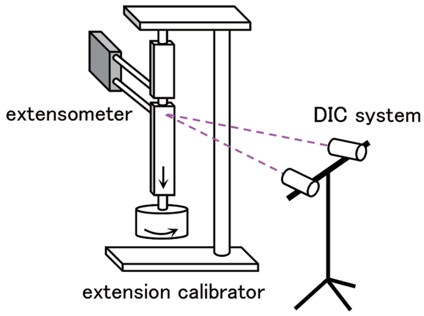

Fig. 5 Verification method of movement amount measurement accuracy at normal temperature

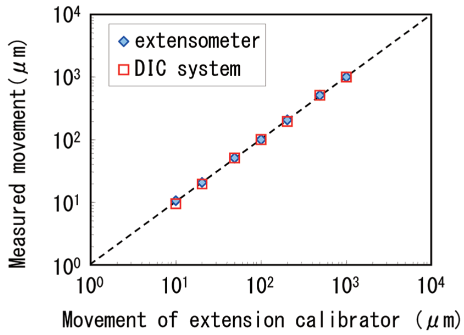

Fig. 6 Verification results of movement amount measurement accuracy at normal temperature

3. Test Results

3.1 Results of accuracy verification of movement amount measurement with DIC system

3.1.1 Results of accuracy verification of movement amount measurement at room temperature

The strain range handled by the thermal strain measurement is as small as several percent or less. The strain must be measured with high accuracy. We verified whether the DIC system can measure the amount of strain that can occur in the exhaust manifold. **Figure 5** shows a method for verifying the accuracy of measuring the movement amount at room temperature. This accuracy was verified by measuring the movement amount on one side of the extension calibrator with the DIC system while measuring the movement amount on the other side of the elongation calibrator with a contact extensometer. The movement amount measurement range was set at 10 to 1 000 μm as is assumed to be applied to actual exhaust manifolds. **Figure 6** shows the results of accuracy verification of the movement amount measurement at room temperature. It was found that the movement amount measured by the DIC system was within the ±3% error range of the movement amount measured with the extensometer in each range. This result confirmed the ability of the DIC system to measure the movement amount with high accuracy.

3.1.2 Results of accuracy verification of thermal expansion measurement during thermal cycling

Photo 1 shows the method of verifying the accuracy of thermal expansion measurement during thermal cycling. An extensometer like that used for measurement at room temperature was attached to a pipe-shaped thermal fatigue test sample. The accuracy of measuring the thermal expansion amount during thermal cycling was verified by measuring the movement amount with the DIC system at the same time. As the thermal fatigue test conditions, the thermal cycling range was set at 200 to 750°C and the load applied to the sample was set to zero, that is, the sample could thermally expand unconstrained.

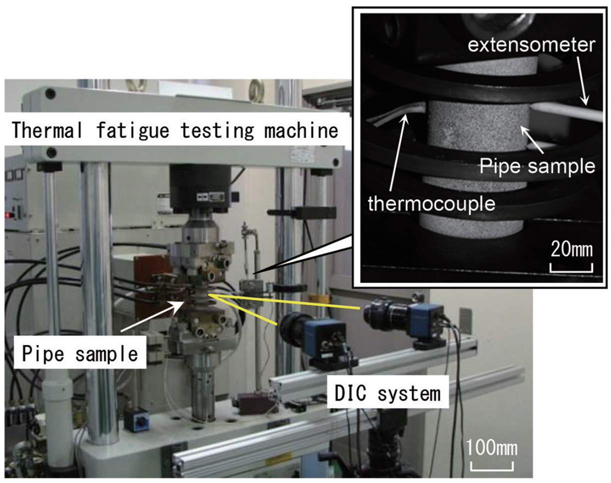

Photo 1 Verification method of thermal expansion amount measurement accuracy during thermal cycling

Figure 7 shows the results of the free thermal expansion amount measured with the extensometer and the DIC system during thermal cycling. The free thermal expansion amount calculated from the linear thermal expansion coefficient is also shown. The free thermal expansion amount in the DIC system was calculated from the difference in the movement amount at two points closest to the tip of the extensometer (gauge length: 15 mm). The free thermal expansion amount in the non-contact strain measurement was within the ±3%

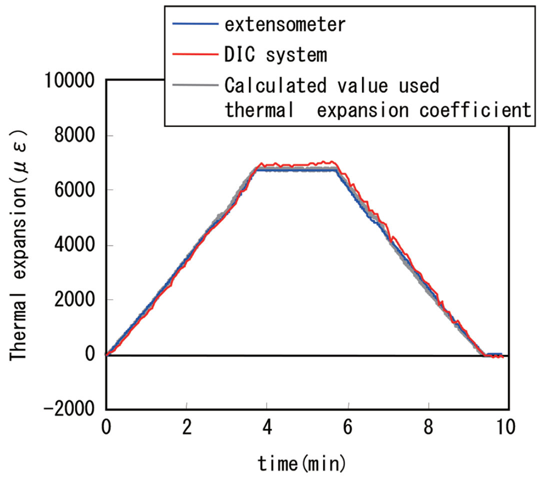

Fig. 7 Measurement results of free thermal expansion amount during thermal cycling

error range of the free thermal expansion amount measured with the extensometer at each temperature. It was confirmed that the thermal expansion amount can be measured with high accuracy during thermal cycling during which the sample surface becomes red hot.

4. Results of Thermal Strain Measurement in Actual Exhaust Manifold

4.1 Results of exhaust manifold temperature measurement

Figure 8 shows the results of measuring the maximum attained temperature of an actual exhaust manifold measured with a thermoviewer. The temperature rose toward the downstream side of the exhaust manifold. The maximum attained temperature increased to about 750°C in the collecting chamber where the exhaust gases from the four ports gather. The temperature in the exhaust manifold flange was 400°C or less. This suggests that the exhaust manifold flanges are more rigid than the exhaust manifold ports. The maximum temperature reached during the engine bench test was also about 750°C. From this, it can be inferred that the temperature distribution in the exhaust manifold including the flange is accurately reproduced by the thermal cycle simulator, although the air blow conditions are different between the actual engine and the thermal cycle simulator.

4.2 Measurement results of thermal strain in exhaust manifold during thermal cycling

Figure 9 shows the results of the thermal strain measured in the exhaust manifold at the maximum attained temperature. The thermal expansion amount increased toward the downstream side of the exhaust manifold according to the temperature distribution. However, the amount of strain applied to exhaust manifold materials cannot be clarified unless it is compared with the amount of free thermal expansion predicted from the temperature rise.

The amount of strain (ε) applied to an exhaust manifold material can be calculated from the linear thermal expansion coefficient (α) of the exhaust manifold material, the temperature difference before and after heating (ΔT), and the measured amount of thermal strain (εm) by the following equation:

$$\varepsilon = \alpha \Delta T - \varepsilon m \quad (1)$$

If ε is positive, it means that compressive strain is produced during heating. That is, it indicates the out-of-phase mode in which heating and strain are reversed in phase. If it is negative, it indicates the in-phase mode in which heating and strain are in phase. In this study, the temperature distribution and the thermal strain distribution are measured at the same time. The strain distribution applied to the exhaust manifold material can be grasped by calculating Equation (1) at each measurement point. The temperature distribution measurements and the thermal strain amount measurements are analyzed using different software. We developed our own software to convert the temperature measurements immediately to the strain amounts applied to the exhaust manifold material by matching the measurement positions.

Figure 10 shows the free thermal expansion amount distribution calculated by multiplying the maximum temperature distribution of the exhaust manifold in Fig. 9 by the linear thermal expansion coef-

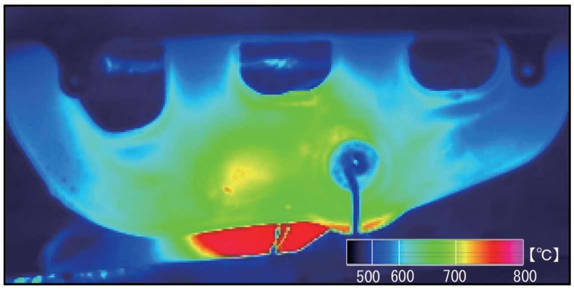

Fig. 8 Measurement results of maximum attained temperature of exhaust manifold

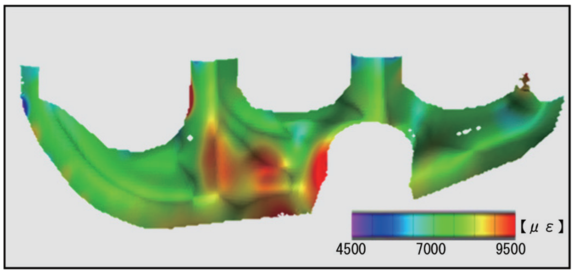

Fig. 9 Thermal strain amount measurement results at maximum attained temperature

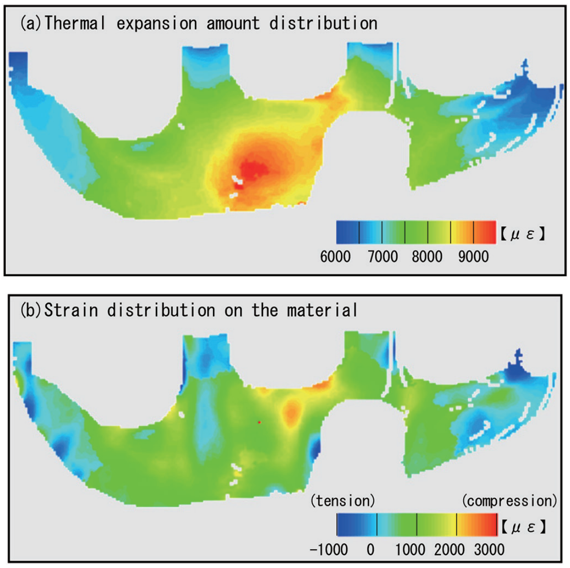

Fig. 10 Thermal expansion amount distribution and strain distribution on the material at maximum attained temperature

ficient at the respective temperatures and by the strain distribution applied to the exhaust manifold material as calculated by Equation (1). Apart from a region showing the maximum temperature in the temperature distribution, another region is recognized where the compressive thermal strain is concentrated in the collecting chamber of the #2 port and the #3 port. A tensile thermal strain region is also confirmed in the upstream of the exhaust manifold. The larger the temperature difference ΔT and the higher the constraint rate, the shorter the thermal fatigue life becomes.[5, 6)] In the measured exhaust manifold, the collecting chamber of the #2 port and the #3 port is estimated as a region likely to suffer thermal fatigue failure. In fact, in the engine bench test conducted separately, wrinkles characteristic of thermal fatigue occurred in the collecting chamber of the #2 port and the #3 port. This shows that the thermal strain measurement technology described here is useful for predicting crack initiation regions. Also, we think that our technology contributes to the improvement in the life prediction accuracy if combined with the relationship between the strain amount applied to the exhaust manifold material and the thermal fatigue characteristics of the exhaust manifold material.

This technology can also measure the thermal strain of components other than exhaust manifolds, such as turbochargers and exhaust gas recirculation (EGR) coolers, as well as their welded joints and other joints if they are visible. In addition, the technology can take pictures through glass. When a part to be measured is covered with glass, the strain in the part can also be measured by the technology. When measuring the thermal strain of the part, it is important to simulate the constraint state of the part. We confirmed that the technology can measure the thermal strain in the exhaust manifold installed in the engine during the bench test. Our technology can thus be widely used.

5. Conclusions

We have developed the technology to simulate the thermal cycling of exhaust manifolds and to measure the thermal strain of the exhaust manifold before and after heating with a non-contact strain measurement unit. The findings we obtained are summarized below.

(1) The accuracy of strain measurement by the digital image correlation method is within ±3% at both room temperature and during thermal cycling. The technology can accurately measure the thermal strain in the exhaust manifold during thermal cycling.

(2) The technology can predict thermal fatigue initiation regions in the exhaust manifold with high accuracy by measuring the temperature distribution and the thermal strain distribution at the same time and by calculating the strain distribution applied to the exhaust manifold materials.

References

1) Oku, M., Nakamura, S., Hiramatsu, N., Uematsu, Y.: Nisshin Steel Technical Report. (74), 26 (1996)
2) Oku, M., Fujimura, Y., Nakamura, S., Ito, K., Nagoshi, T., Uematsu, Y.: Nisshin Steel Technical Report. (80), 32 (2000)
3) Tomita, T., Oku, M.: Nisshin Steel Technical Report. (90), 30 (2009)
4) Hamada, J., Hayashi, A., Kanno, N., Komori, T., Ito, K., Fukuda, N., Inoue, N.: Materia Japan. 56, 33 (2017)
5) Oku, M., Fujimura, Y., Nagoshi, T.: CAMP-ISIJ. 13, 1173 (2000)
6) Oku, M., Nakamura, S., Hiramatsu, N., Uematsu, Y.: Nisshin Steel Technical Report. (66), 37 (1992)

Kazunari IMAKAWA
Senior Researcher
Materials Reliability Research Lab.
Steel Research Laboratories, R & D Laboratories
Nippon Steel Corporation
20-1 Shintomi, Futtsu City, Chiba Pref. 293-8511

Yoshihiro OKA
Researcher
Plate, Bar & Wire Rod Research & Development Div.
Research & Development Center
Nippon Steel Stainless Steel Corporation

Manabu OKU
General Manager
Function Creation Research & Development Div.
Research & Development Center
Nippon Steel Stainless Steel Corporation